



17th International Conference on Sheet Metal, SHEMET17

The Effects of process parameters on mechanical properties and corrosion behavior in friction stir welding of aluminum alloys

D'Urso, G.^a *; Giardini, C.^a; Lorenzi, S.^b; Cabrini, M.^b; Pastore, T.^b

^aUniversity of Bergamo – DIGIP – Viale Marconi 5, Dalmine (BG) - Italy

^bUniversity of Bergamo – DISA – Viale Marconi 5, Dalmine (BG) - Italy

Abstract

The present study was carried out to evaluate how the process parameters affect the mechanical properties and the corrosion behavior of joints obtained by friction stir welding (FSW). The experimental study was performed by means of a CNC machine tool for the friction stir welding of two aluminum alloys, namely AA7075 and AA2024, taking also into account the combination between the two materials. The joints were executed varying the process parameters, namely rotational speed and feed rate. Tensile tests and hardness tests were carried out to evaluate the mechanical properties of the joints. The corrosion behavior of welded specimens was analyzed by means of local free corrosion potential measurements to determine anodic and cathodic areas of welds. The results evidenced that the low hardness areas have the free corrosion potential more anodic than the nearest zones. The differences of potential between the different areas of the welding have the consequence of galvanic corrosion of the less noble area. The location and the extension of the anodic areas depend both on the alloy and on the welding parameters. The preferential corrosion of these areas were confirmed by means of long time immersion tests. The attacks morphology depends on the alloy: in AA2024 a severe crevice and pitting attack takes place, whereas the AA7075 shows exfoliation corrosion along the rolling bands. Coupling the two different alloys, a severe galvanic attack takes place on the AA7075, in the correspondence of the lower hardness areas. The decreasing of hardness and the different electrochemical behavior in the correspondence of the welding were due to the microstructural alteration of the alloys during the FSW. The correlation between process parameters and joints properties allowed to identify the most suitable welding conditions.

© 2017 Published by Elsevier Ltd. This is an open access article under the CC BY-NC-ND license (<http://creativecommons.org/licenses/by-nc-nd/4.0/>).

Peer-review under responsibility of the organizing committee of SHEMET17

Keywords: FSW, Aluminum alloys; Process parameters, Corrosion behavior.

* Corresponding author. Tel.: +39-338-2052330; fax: +39-035-2052043

E-mail address: gianluca.d-urso@unibg.it

1. Introduction

When joining difficult to be welded materials (such as Al, Ti and Mg alloys but also Advanced High-Strength Steel [1]), it is possible to refer to Friction Stir Welding (FSW) technology (patented by TWI in 1991 [2, 3]). FSW has recently received large attention from automotive and transportation [4], aeronautical [5], in-white and other industrial sectors. Using this technology, it is also possible to join dissimilar materials [6-8] in several configurations.

The FSW process gives rise to large plastic flow and heat generation that determine remarkable microstructural modifications, resulting in local changes of material mechanical characteristics. In particular, moving from the periphery of the joined parts (base material - BM, without metallurgical modifications) towards the pin axis, a heat affected zone (HAZ) is initially found; in this zone the material undergoes to temperature increase that modifies microstructure and mechanical properties. Moving towards the pin axis, the thermo-mechanically affected zone (TMAZ), where the material is heavily plastically deformed by the tool stirring action, can be observed. Finally, in the nugget, located in the middle of the joint, there is a recrystallized area where fine grains of uniform size replace the original grains [9,10]. For this reason, it is very important to understand the effects of process parameters and process setup on the weld quality and strength in terms of material microstructure and material mechanical properties.

The FSW process is gaining importance especially for high resistance aluminum alloys (for example AA2024 and AA7075 are of great interest because of their aeronautical use), which are difficult to be joined with traditional techniques which alter the microstructure obtained during age hardening. Several Authors studied these aspects with particular attention to the quality of FSW joints in terms of mechanical properties (UTS, fatigue resistance etc.) [11-12]. In addition, particular attention has to be paid due to the well-known susceptibility of the alloy to stress corrosion cracking [13]. Despite the enhanced properties, the added elements introduce higher degree of heterogeneity especially evident in high strength Al alloys due to the presence of secondary phases or termed constituent particles [14]. Corrosion behavior can be mainly affected by the presence – size and distribution – of such phases, modifying the anodic and cathodic behavior of the zones of joining. [15,16]. Several works describing corrosion morphologies that can occur also concomitantly in form of localized corrosion, e.g., galvanic corrosion, pitting, dealloying or intergranular attack [17-19] were found, but very few data regarding the combination of different alloys and the systematic correlation between mechanical properties and corrosion behavior can be noticed. Under such considerations, the corrosion behavior can be significantly influenced by welding parameters and a strict correlation between them and alloy macro and microstructure has to be further investigated [20].

2. Experimental set up

2.1. FSW set up

The experimental analysis was performed by means of a CNC machine tool. Butt joints were obtained on sheets having a thickness equal to 4 mm. Two different aluminum alloys, namely AA2024-T3 and 7075-T6 were used for this purpose and the joints were executed with three different combination of materials: AA2024 – AA2024, AA7075 – AA7075, AA7075 – AA2024. Table 1 shows the mechanical properties of the materials. Sheets of 200 x 80 mm were welded by using tools with smooth plane shoulder (16 mm diameter) and pin having a frustum of cone shape (pin maximum and minimum diameters equal to 6 and 4 mm, pin height equal to 3.8 mm). The welding operations were carried out by varying tool rotational speed ($S=1000, 1500, 2000$ rpm) and feed rate ($F=10, 35, 60$ mm/min). Three welding repetitions were carried out for each combination of parameters.

2.2. Mechanical characterization of the joints

A universal testing machine Galdabini with a load cell of 50 kN was used to evaluate the mechanical properties of the FSW joints as a function of the different process parameters. Tensile tests were performed orthogonally to the welding direction according to UNI EN 10002-1:2004 on specimens with 160 x 20 mm, having the welding nugget placed in the middle of gage length. Tests were carried out under speed control (7.6 mm/min) on 3 specimens for

each welding condition. A pre-load equal to 0.5 kN was set for all the tests. In order to evaluate the influence of process parameters on both the material structure and the joint strain hardening, the microhardness distribution of the welded sections were evaluated in all the tested conditions.

Table 1. Mechanical properties.

Mechanical properties	AA2024	AA7075
Yield strength [MPa]	345	511
UTS [MPa]	459	578
Max strain [%]	17	11

Micro-Vickers tests were carried out using a load of 2 N and a permanence time equal to 15 seconds. A grid composed by three lines of indentations (moving from a distance of 1 mm to a distance of 4 mm from the upper surface) was executed on each specimen. On each line the distance among the indentations was equal to 3 mm. The tests were executed moving from the joint axis to the base material until the hardness of the base material was reached.

2.3. Corrosion tests

Local corrosion potential measurements and four-point bending tests have been performed to evaluate the corrosion behaviour and stress corrosion cracking susceptibility of FSW Joints. The tests were performed on 4x20x160 mm prismatic specimens obtained by FSW joints of the same alloy (7075-7075 and 2024-2024) and mixed joints (7075-2024). Several processing parameters were studied: feed rates of 10-35 mm/min and tool speed of 1000-1500 rpm. The specimens were polished by emery papers up to 1000 grit and degreased in acetone in ultrasonic bath for 5 minutes. After polishing, the specimens were stored in still air for 48 hours to allow the formation of the natural protective film. Free corrosion potential measurements have been carried out by moving a 1 mm capillary equipped with a Standard Calomel Electrode (SCE) over the specimen length every 10 mm. The specimens were pre-soaked for 48 hours in distilled water to achieve stable potential values. The potential profile was obtained in the central zone of the specimen to avoid border effects. The specimens were covered by a thin layer of distilled water to permit the execution of the potential measurements. Four-point bending tests have been performed by using the bending device shown in Fig. 1, according to ASTM G39. The specimen is put inside the bending device to attain uniform tensile strain distribution over the welded surface. The specimens were loaded up to the 80% of the tensile strength of FSW joints derived by tensile tests. Four glass cylinders were used to avoid galvanic coupling between the stainless steel specimen holder and aluminium. The specimens were exposed in a cell filled with about 30L water with 35 g/L sodium chloride for more than 40 days. At the end of the exposure tests, the specimens were unloaded, washed in distilled water and rinsed with acetone in ultrasonic bath. The surfaces were then observed by means of optical microscope up to 600 magnifications and scanning electron microscope equipped with energy dispersive x-ray analysis.

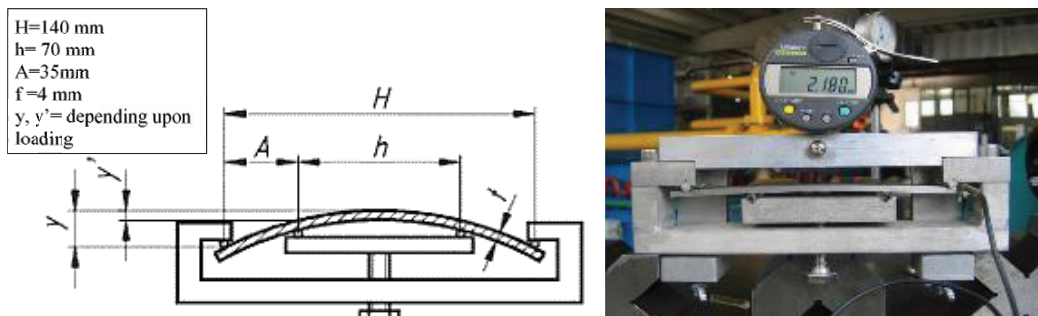


Fig. 1. Four-point bending device (a) geometry (b) loading phase.

3. Analysis of the results

3.1. Mechanical properties

Fig. 2 resumes the results of both tensile and hardness tests. In particular, the diagrams on the left column show the interaction plots of the UTS as function of feed rate for the different values of tool rotational speed. Each marker corresponds to the average of 3 values obtained in the same experimental conditions.

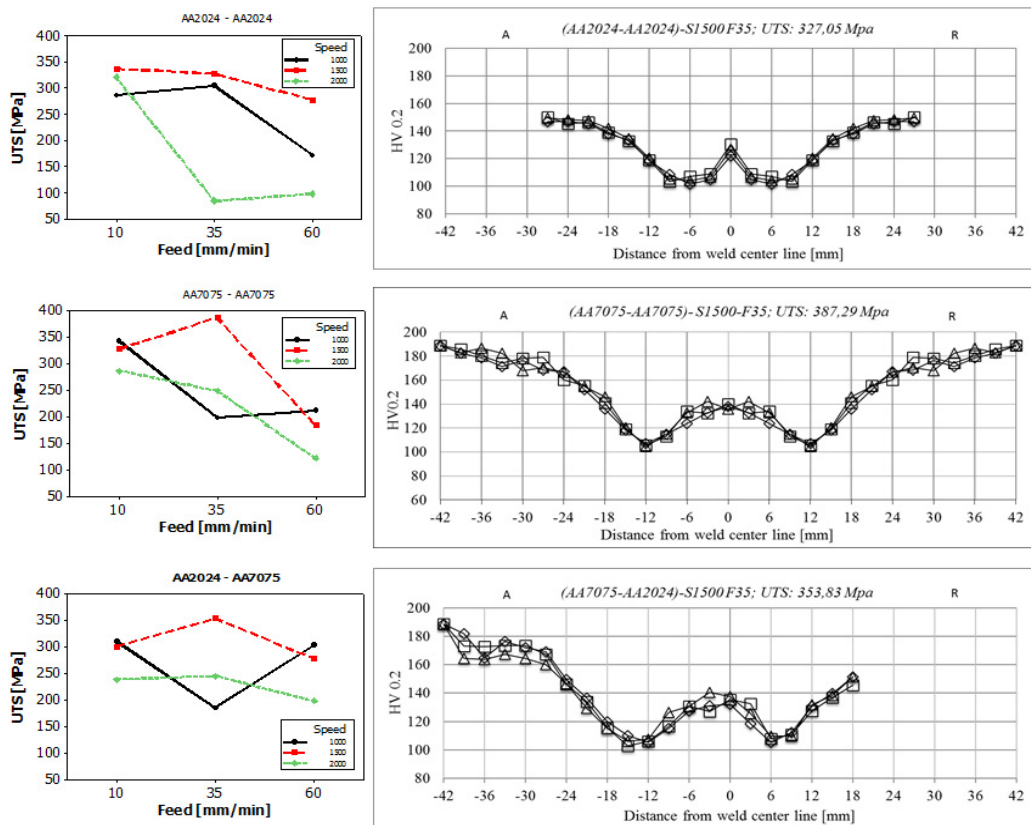


Fig. 2. Interaction plots for UTS and microhardness profiles as function of feed rate and rotational speed for AA2024 and AA7075.

The best condition in terms of mechanical strength was obtained using the intermediate values of rotational speed, equal to 1500 rpm; the intermediate value of feed rate can be also considered an optimal condition. As a general remark, it is possible to affirm that the best conditions in terms of UTS are achieved when the process parameters result in low values feed rate per unit revolution (F/S), that means a higher thermal contribution to the joint region. The microhardness distributions measured on the joint section for the three combination of materials in the intermediate process condition (speed 1500 rpm, feed 35 mm/min) are also reported in Fig. 2 (right column).

The hardness in the welded region is significantly lower with respect to the base material (146 μ HV for AA2024 189 μ HV for AA 7075). The high temperature achieved during the FSW process can be considered as the major cause of this softening effect. Even just a few microhardness diagrams are reported for reasons of synthesis, it is possible to assert that the width of the softened region and the microhardness values recorded in the same region are influenced by the welding process parameters. In particular, an increase in thermal contribution (e.g. high rotational speed and low feed rate) results in wider softening region and lower values of hardness. On the contrary, a significant reduction of width can be noticed when high values of F/S ratio are concerned.

3.2. Corrosion behavior

The results of local free corrosion potential measurements to distinguish anodic and cathodic areas of welds are shown in Fig. 3. As a title of example, data on 7075 aluminum alloy and 2024 welded joint are reported. The results evidenced that the lower the hardness, the more anodic the corrosion potential. In presence of such differences in the free corrosion potential, galvanic corrosion of the less noble area can occur. Such effect is emphasized in the case of mixed welding, in which 7075 alloy is joined with 2024 alloy. The position and the extension of the anodic areas depend both on the alloy and on the welding parameters. The presence of preferential corrosion sites was confirmed also by means of long time immersion tests (Fig. 4). The attacks morphology is strictly dependent upon the alloy. AA2024 shows a severe pitting attack mainly in correspondence of the zones of the nugget, whilst AA7075 alloy shows exfoliating corrosion - mainly along the rolling bands – in correspondence of the thermo-mechanical affected zone. The coupling the two different alloys causes a severe galvanic attack mainly in thermo-mechanical affected zones on the AA7075 alloy, in the correspondence of the areas with lower hardness. The corrosion behavior modifies in function of welding parameters and a certain effect of both speed and feed rate can be noticed. The decreasing of hardness and the different electrochemical behavior in the correspondence of the welding were due to the microstructural alteration of the alloys during the FSW. The presence of precipitates (mainly copper and zinc) with different size and distribution significantly varies along the welding, as proved by SEM and EDX analysis (Fig. 5).

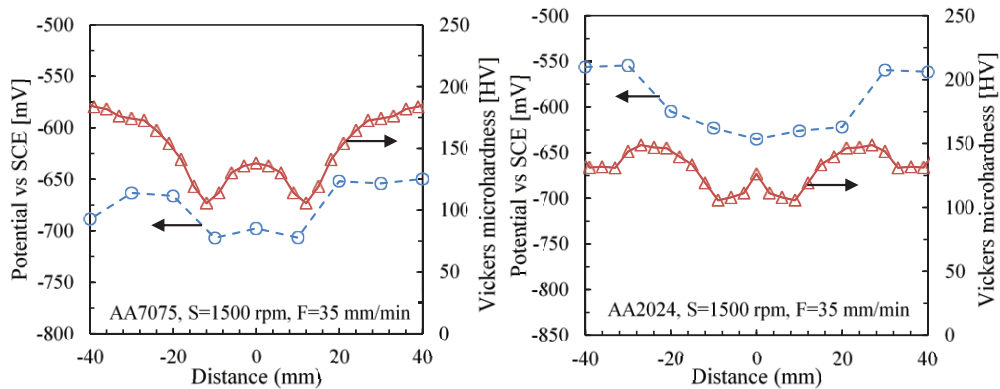


Fig. 3. Vickers hardness profile and local free corrosion potential values along the FSW joint.

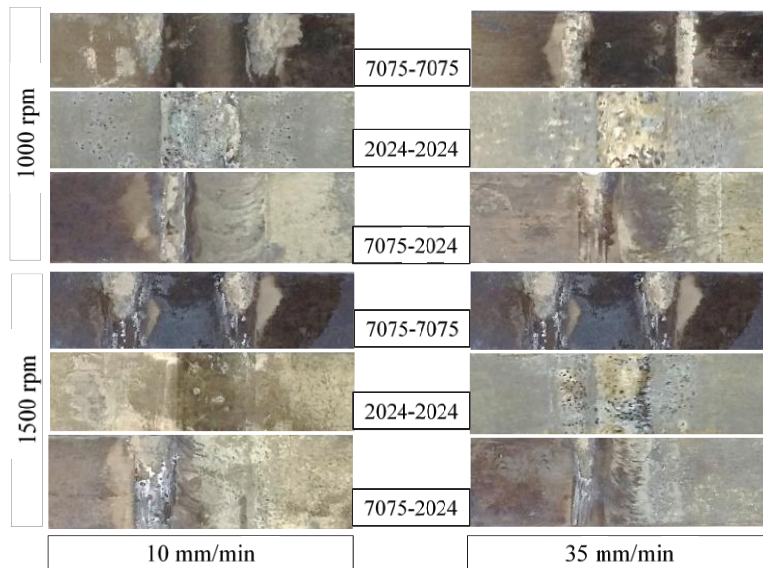


Fig. 4. Effect of speed and feed rate on the corrosion morphologies of FSW joints.

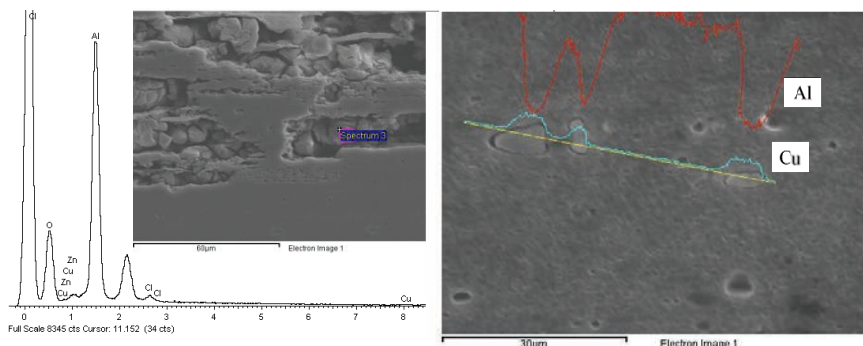


Fig. 5. SEM and EDX spectrum of precipitates in the thermo-mechanical affected zone of AA7075 FSW joint (left); composition profiles in the zones in proximity of the nugget of AA2024 FSW joint (right).

4. Conclusive remarks

The mechanical properties of FSW joints of AA2024 and AA7075 aluminum alloys have been analyzed and the correlation between process parameters and joints properties allowed to identify the most suitable welding conditions.

The attacks morphology depends on the alloy: in AA2024 a severe crevice and pitting attack takes place, whereas the AA7075 shows exfoliation corrosion along the rolling bands. Coupling the two different alloys, a severe galvanic attack takes place on the AA7075, in the correspondence of the lower hardness areas. The decreasing of hardness and the different electrochemical behavior in the correspondence of the welding were due to the microstructural alteration of the alloys during the FSW.

References

- [1] K. Martinsen, S.J Hu, B.E Carlson, Joining of dissimilar materials, CIRP Annals - Manufacturing Technology 64 (2015) 679-699.
- [2] W.M. Thomas, E.D. Nicolas, J.C. Needham, M.G. Murch., P. Templesmith, C.J Dawes, Int.l patent Application, 1991, No.PCT/GB92/02203.
- [3] W.M. Thomas, E.D. Nicolas, J.C. Needham, M.G. Murch., P. Templesmith, C.J Dawes, US Patent Application, 1995, No. 5460317.P.L.

- [4] T. Kawasaki, T. Makino, S. Todor, H. Takai, M. Ezumi, Y. Inada, Application of Friction Stir Welding to the Manufacturing of Next Generation A-train Type Rolling Stock, Proceedings of 2nd international symposium on Friction stir welding, Gothenburg, Sweden, 2000.
- [5] D. Lohwasser, Application of Friction Stir Welding for aircraft industry, Proceedings of 2nd int. symp. on FSW, Gothenburg, Sweden, 2000.
- [6] E.Taban, J.E.Gould, J.C.Lippold, Dissimilar Friction Stir Welding of 6061 T6 Aluminium and AISI 1018 Steel: Properties and Microstructural Characterization, *Material & Design* 31 (2010) 2305-2311.
- [7] H. Uzun, C. Dalle Donne, A. Argonotto, T. Ghidini, C. Gambaro, Friction Stir Welding of Dissimilar Al 6013.T4 to X5CrNi18-10 Stainless Steel, *Materials & Design* 26 (2005) 41-46.
- [8] T. Watanabe, H. Takayama, A. Yanagisawa, Joining of Aluminium Alloy to Steel by Friction Stir Welding, *JMPT* 178 (2006) 342-349.
- [9] P. Fanelli, F. Vivio, V. Vullo, Experimental and numerical characterization of FSSW joints, *Eng. Fract. Mech.* 81 (2012) 17-25.
- [10] K.V. Jata, S.L. Semiatin, Continuous dynamic recrystallization during friction stir welding of high strength aluminum alloys, *Scripta Materialia* 43 (2000) 743-749.
- [11] S.A. Khodir, T. Shibayanagi, FSW of dissimilar AA2024 and AA7075 aluminum alloys, *Mat. Sci. and Eng. B* 148 (2008) 82–87.
- [12] P. Avinash et al., Friction stir welded butt joints of AA2024 T3 and AA7075 T6 aluminum alloys, *Procedia Engineering* 75 (2014) 98–102.
- [13] C. Vargel, M. Jacques, M.P. Schmidt, The most common wrought aluminium alloys, in: C.V.J.P. Schmidt (Ed.), *Corrosion of Aluminium*, Elsevier, Amsterdam, (2004) 61–69.
- [14] K.A. Yasakau, J. Tedim, M.F. Montemor, A.N. Salak, M.L. Zheludkevich, M.G.S.Ferreira, Mechanisms of localized corrosion inhibition of AA2024 by ceriummolybdate nanowires, *J. Phys. Chem. C* 117 (2013) 5811–5823.
- [15] N. Birbilis, R.G. Buchheit, Electrochemical characteristics of intermetallicphases in aluminum alloys-an experimental survey and discussion, *J.Electrochem. Soc.* 152 (2005) B140–B151.
- [16] F. Andreatta, H. Terryn, J.H.W. de Wit, Corrosion behaviour of different tempers of AA7075 aluminium alloy, *Electrochim. Acta* 49 (2004) 2851–2862.
- [17] L. Threadgill, A.J. Leonard, H.R. Shercliff & P.J. Withers Friction stir welding of aluminium alloys, *Int. Mat. Reviews*, 54:2 (2009) 49-93.
- [18] K.D. Ralston, J.G. Brunner et al., Effect of Processing on Grain Size and Corrosion of AA2024-T3, *Corrosion* (67) 10, 105001-1-10.
- [19] J.B. Lumsden, M.W. Mahoney, G. Pollock, and C.G. Rhodes, Intergranular Corrosion Following Friction Stir Welding of Aluminum Alloy 7075-T651, *Corrosion* (55) 12, 1127-1135.
- [20] M. Jariyaboon, A.J. Davenport, R. Ambat, B.J. Connolly, S.W. Williams, D.A. Price, The effect of welding parameters on the corrosion behaviour of friction stir welded AA2024–T351 *Corrosion Science* 49 (2007) 877–909.